Time-resolved measurements of nonthermal x-ray emission of Ti XXI lines in electron-cyclotron-heated tokamak plasmas

P. Lee and A. J. Lieber
GA Technologies Inc., P.O. Box 85608, San Diego, California 92138

A. K. Pradhan and Yueming Xu
Joint Institute for Laboratory Astrophysics, University of Colorado and National Bureau of Standards, Boulder, Colorado 80309-0440

(Received 5 May 1986)

Observations of the heliumlike titanium spectra with 20-ms temporal resolution during electron cyclotron heating (ECH) of Doublet III tokamak plasma have been made. Several prominent lines in the heliumlike spectra are observed: $1s^2\,{}^1S_0 \leftarrow 1s\,2p\,{}^1P_1$ (labeled w), $1s^2\,{}^1S_0 \leftarrow 1s\,2p\,{}^3P_{1,2}$ (y,x), and $1s^2\,{}^1S_0 \leftarrow 1s\,2s\,{}^3S_1$ (z). In addition, the dielectronic satellite lines from the autoionizing lithiumlike ionization states are also observed, e.g., $1s^2 2p\,{}^2P^\circ_{3/2} \leftarrow 1s\,2p^2\,{}^2D_{5/2}$ (j), $1s^2 2s\,{}^2S_{1/2} \leftarrow 1s\,2p\,2s\,{}^2P^\circ_{3/2}$ (q), etc. The intensity of the resonance line w (i.e., $1s^2\,{}^1S_0 \leftarrow 1s\,2p\,{}^1P_1$) is found to be extremely sensitive to the ECH power. Ion temperatures rise from the Ohmic phase to steady-state ECH phase in 20–40 ms at an electron density of 6×10^{13} cm^{-3}. Time-resolved line ratios $G=(x+y+z)/w$, $R=z/(x+y)$, and j/w are also presented. Detailed analysis of the observed spectra is carried out, based on the relevant atomic and plasma effects, and it is concluded that there exists a significant departure from a Maxwellian distribution of electrons in the present ECH plasmas, which are also dominated by nonequilibrium ionization.

I. INTRODUCTION

Electron cyclotron heating (ECH) of plasmas is being explored as a possible method of auxiliary heating of tokamaks to thermonuclear conditions. Recent availability of high-power, long-pulse-length gyrotrons have made ECH experiments feasible on large tokamak devices.[1] ECH is an electron-wave interaction phenomenon whereby radio-frequency electromagnetic waves resonantly transfer their energies to electrons in cyclotron orbits in a magnetized plasma. The energetic electrons then heat the ions through electron-ion collisions. An advantage of ECH is the localized nature of wave absorption, with the position of resonance dependent only on the magnitude of the local magnetic fields; thus control of current density and electron temperature profiles can be accomplished by adjustment of toroidal magnetic fields. The disadvantages of ECH are the indirect heating of ions through electrons and that the electron energy distributions are expected to be non-Maxwellian.

Much of the effort in the study of ECH, both experimental and theoretical, is in the area of bulk plasma effects,[1–5] such as energy confinement times and scaling, and comparison to neutral-beam injection heating. On the other hand, the effects of ECH on the characteristic line emissions from tokamak plasmas have not received much attention. High-resolution spectroscopy has been shown to be a powerful technique in the study of astrophysical plasmas[6] and laboratory plasmas.[7–10] Parameters such as electron and ion temperatures, ion motions, and ionization conditions can be deduced from high-resolution x-ray spectroscopy of hot plasmas. Furthermore, ECH power applied to tokamak discharges is turned on or off in a few milliseconds, and the durations of the ECH power and stable discharges are greater than 100 ms. This effect might be useful. in the study of transient spectra such as the sudden temperature jump model of Mewe *et al.* for solar flares.[11]

Reports of high-resolution x-ray spectra generated during ECH of tokamak plasmas are scarce. Bryzgunov *et al*[12] have made measurements of heliumlike chromium line radiation in the wavelength band of 2.19 Å on the T-10 tokamak. The dispersive element of the spectrograph was a bent quartz crystal cut along the (1340) plane and arranged in a 50-cm radius of curvature Johann mount. The detection scheme consisted of converting x rays to visible light through the use of K-51 luminor converter plate, and subsequent intensification of the visible light before recording on photographic films. The spectral resolution $\lambda/\Delta\lambda$ of the instrument was about 3300. 500 kW of ECH power was applied for 50 ms to tokamak plasmas with typical parameters of 250 kA of Ohmic current and electron density of $(2-3)\times10^{13}$ cm^{-3}. Nine plasma discharges of 50 ms each centered on the ECH were needed to record a chromium spectrum.

In this paper we report the observation of heliumlike titanium spectra with 20 ms temporal resolution during high-power injection of ECH of up to 250 ms pulse length into the Doublet III tokamak. The emphasis here is on the time-dependent nature of the spectral lines and their relevant ratios.

ECH experiments were carried out with toroidal magnetic fields of $1.8<B_T<2.4$ T, plasma current of $300<I_P<1\,800$ kA, plasma elongation of $1.4<\kappa<1.6$, and central electron density of $1\times10^{13}<n_e<10\times10^{13}$ cm^{-3}. The volume of the plasma is 8.5 m^3 with major ra-

dius $R \sim 143$ cm and minor radius $a \sim 40$ cm. Six VGE-8006 gyrotrons operating at 60 GHz generate up to 1 MW of rf power for pulse duration of up to 500 ms, although the typical pulse length was 250 ms. The plasma cutoff density for wave propagation is $\bar{n}_e = 5.6 \times 10^{13}$ cm^{-3} and the resonant magnetic field is 2.14 T. The extraordinary wave propagates at an angle of 30° to the radial, from the inside wall of the tokamak, and the rf power is fully absorbed in an area roughly 10 cm in height and 5 cm in the radial direction centered near the resonance.

The spectrometer used in this experiment is a Johann-geometry Bragg crystal spectrograph constrained to a 3-m Rowland circle. A curved quartz crystal cut along the $(20\bar{2}\,\bar{3})$ plane with a $2d$ spacing of 2.75 Å diffracts and forces x rays onto a position-sensitive delay line gas proportional counter with a spatial resolution of 200 μm. The resolving power of this instrument, $\lambda/\Delta\lambda$, is 19 000.

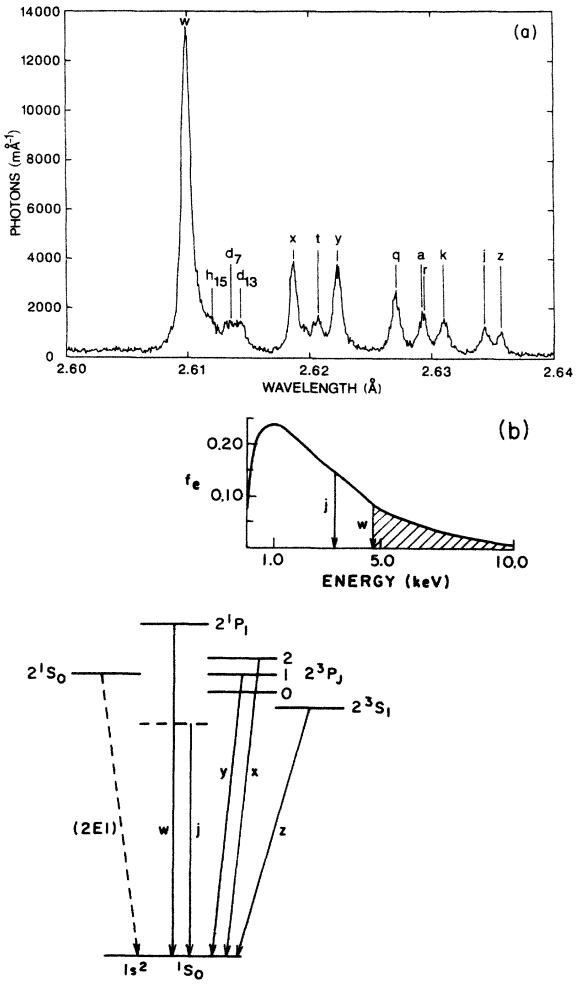

FIG. 1. (a) Typical Ti XXI spectra with 200 ms integration time measured during electron cyclotron heating of moderate central density (5.91×10^{13} cm^{-3} in this case) plasma. The prominent lines have been labeled. (b) Term diagram for the He-like spectrum for lines observed in this experiment. The excitation of the w line can be achieved for electrons with kinetic energy above 4.75 keV (as shown by the shaded region) whereas the j line can be excited only by electrons in an extremely narrow band ($< 10^{-4}$ keV).

The data are acquired in 15 times segments of nominally 20 ms per segment. A detailed description of this instrument can be found elsewhere.[13] The spectrometer views the tokamak discharge tangentially; thus the combination of this long view chord through the center of the plasma with the high temperature observed in the center of the plasma ensures that the contribution from the cooler outer edges of the discharge in insignificant.

II. OBSERVATIONS

Titanium impurity radiation in the wavelength band of 2.60–2.64 Å [shown in Fig. 1(a)] is representative of our moderate-density ECH discharges. The relevant discharge parameters are $I_P = 501$ kA, $B_T = 2.142$ T, and 550 kW of ECH power injected. The central electron temperature and density measured by Thomson scattering near the end of the ECH pulse are 1.71 keV and 5.91×10^{13} cm^{-3}, respectively. Detailed analysis of the heliumlike titanium spectra has been reported earlier.[14] Briefly, the prominent heliumlike lines are the resonance line w, the intercombination lines x and y, and the forbidden line z; they derive from the transitions $1\,^1S_0 - 2\,^1P_1$, $1\,^1S_0 - 2\,^3P_{2,1}$, and $1\,^1S_0 - 2\,^3S_1$, respectively, as shown in Fig. 1(b). The observed satellite lines with $n = 2$ spectator electron transitions are t, q, a, r (unresolved), k, and j; the $n = 3$ dielectronic recombination satellite lines are h, d_7, and d_{13}.

The line brightness of w is plotted in Fig. 2(a) for the discharge discussed above. A change in line intensity by a factor of 5 within the 20-ms resolution of our instrument is typical of moderate-density ECH discharges. The power delivered to the plasma is also shown in the figure. The onset of ECH is clearly evident, with dramatic increases in the intensities of all the lines from the Ohmic phase, particularly the line w. The amplitude of the observed spectral lines responded to the ECH power in a time less than the temporal resolution of the instrument. Computer simulations have predicted that the electron temperature increased from 0.7 to 1.9 keV in 2 ms.[15] This is consistent within the limit of our resolution. Ion temperature deduced by the Doppler-broadened width of the resonance line w shows a modest rise from 0.7 keV to about 1 keV during ECH [see Fig. 2(b)]. The electron temperature for this discharge on the other hand is much higher than the ion temperature (1.71 keV at 900 ms).

For the purpose of comparison we show results of a high-density ECH discharge in Fig. 2(b). Electron temperature of 0.79 keV and electron density of 15.6×10^{13} cm^{-3} is obtained with $I_P = 490$ kA, $B_T = 2.142$ T, and ~ 450 kW of ECH injection. The intensity of the resonance line becomes measurable about 75 ms after initiation of ECH. The corresponding ion temperature is 1 keV [similar to that in Fig. 1(a)]. It is interesting that ECH is able to heat the plasma when the electron density is clearly beyond the classical cutoff of the plasma.[2] Some theoretical analysis has been done to explain this effect.[16] The electron and ion temperatures are equal within the limit of the measurements at 900 ms.

Gaussian fits to the spectral lines were made for each 20-ms time slice from which the diagnostic line ratios

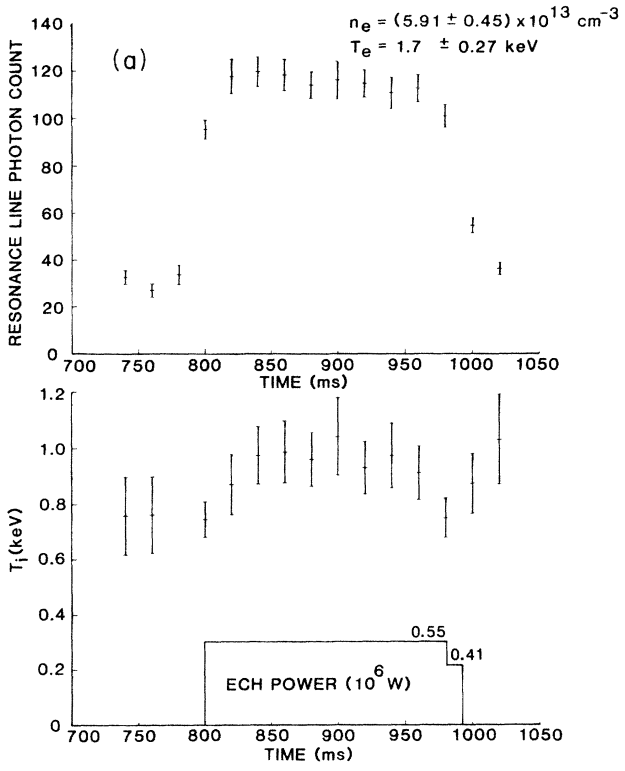

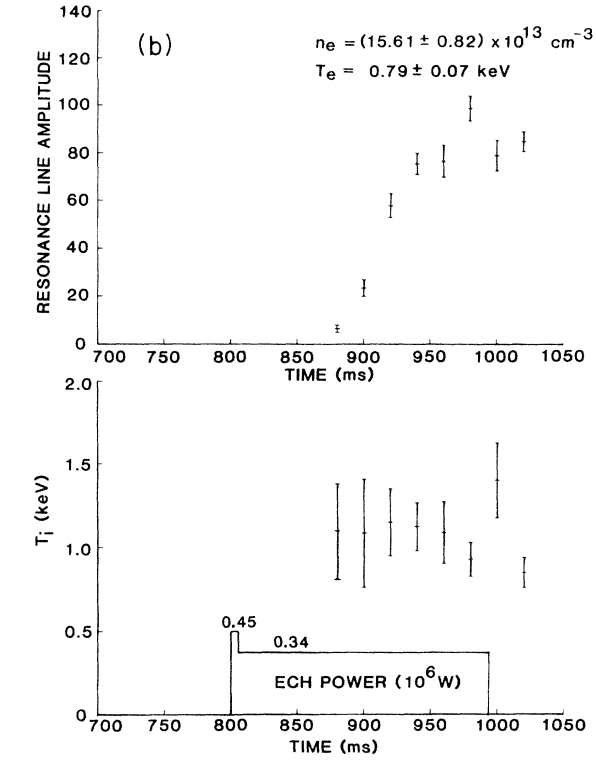

FIG. 2. (a) Line brightness for the resonance line w and ion temperature as a function of time for moderate density discharge $n_0 = 5.91 \times 10^{13}$ cm^{-3}. (b) Line brightness for the resonance line w and ion temperature for an overdense plasma $n_0 = 15.61 \times 10^{13}$ cm^{-3}. In this case plasma heating is achieved even in the overdense case.

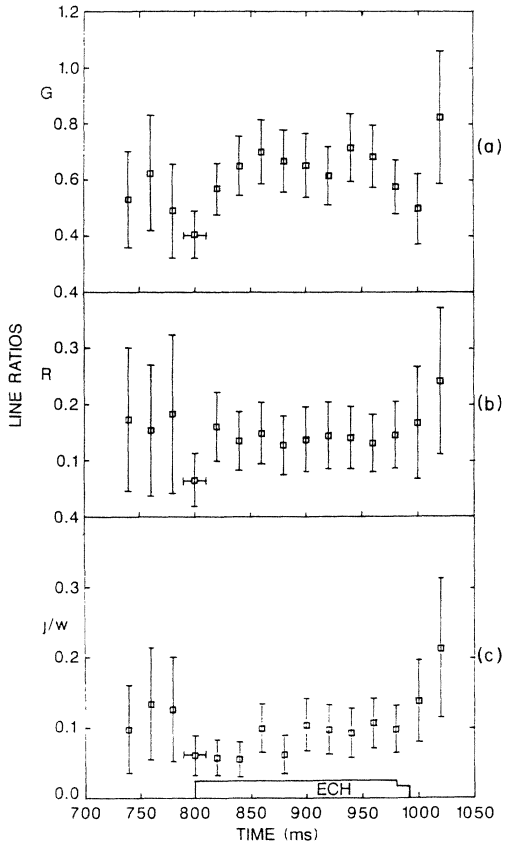

FIG. 3. (a)–(c) Line ratios $G \equiv x + y + z/w$, $R \equiv z/x + y$, and j/w are measured as a function of time. The onset of ECH is clearly evident by the drop in all the line ratios. 20 ms temporal resolution is indicated for the 800-ns data point.

$G = (x + y + z)/w$, $R = z(x + y)$, and j/w were determined. The common feature of the time-dependent line ratios shown in Fig. 3 for the discharge of Fig. 1(a) is at 800 ms (initiation of ECH) where all the ratios exhibit a sudden decrease at the onset of ECH, followed by a rise to more stable values. This is a general characteristic of ECH spectra; the variations are much sharper, and these line ratios are much lower, than in other forms of plasma heating, viz., Ohmic. The underlying population mechanism is clearly affected by the ECH. In Sec. III we discuss the observations in detail.

III. INTERPRETATION OF THE Ti XXI ECH SPECTRA

The principal and the dielectronic satellite lines of the spectra of He-like ions have been the subject of a number of theoretical and experimental studies and it is well recognized that the variations in the intensities of these lines provide very useful information on the temperature, density, state of ionization imbalance, and the electron distribution function in the plasma.[17–19]

The observed spectrum in Fig. 1(a) shows several features that appear to be characteristic of ECH plasmas. The foremost among these is the predominance of the w

line, over all other lines in the spectrum, to a much greater extent than in Ohmically heated plasmas,[14,20] and in plasmas usually present in astronomical sources.[21] The other features are a very small intensity in the z line, particularly relative to the x and y lines, and weak intensities of the dielectronic satellite lines, e.g., j and k, relative to the w. This last feature is especially interesting since it can be related to the fractional nonthermal content of the electron distribution.[22,23] In the present analysis we approach the problem of determining the extent of departure from a Maxwellian in several different ways. The theoretical methods employed and the results are described in the next section.

A. The dielectronic satellite to resonance line ratio: j/w

The consideration of the nonthermal component in the electron distribution usually implies that a small fraction of the electrons are accelerated to velocities much higher than given by the bulk temperature of the plasma. To a first approximation one may treat the distribution as a bi-Maxwellian with the bulk temperature T_1 and the higher component at T_2. For $T_1 \sim 1$–2 keV, as in the present case, one expects T_2 to be at least a few times T_1 and the high-energy part of the Maxwellian distribution to be enhanced. The excess high-energy electrons would then result in enhanced electron impact excitation rates for some atomic transitions, particularly for optically allowed transitions since the cross sections for dipole transitions are affected to a large extent by the large angular momenta of the high-energy electrons. Thus for the He-like ions one expects the w transition to be enhanced, relative to other transitions, by the nonthermal high-energy component. On the other hand, the dielectronic satellites are excited only by the electrons at precisely the energy of the particular autoionizing levels (to within the autoionization width of the levels) and therefore the satellite intensities are unaffected by the excess high-energy tail.[22,23] It has been pointed out by Inokuti[24] that for electron impact excitation with energies greater than about 5 keV one should account for the relativistic effects in the calculation of the cross sections. The relativistic Coulomb-Bethe formula given by Fano is used by Bartiromo *et al.*[23] in order to calculate the rate coefficient for the w transition in Fe XXV. A very useful fact discussed by Bartiromo *et al.* is that the rate coefficient can be considered to be approximately a constant for the electrons in the high-energy tail of the distribution ($E > 20$ keV for Fe XXV).

The usual expression for ratio of the dielectronic satellite to the resonance line for the nonrelativistic, Maxwellian case is

$$D_{\text{theor}} = \frac{q(s)}{q(w)} = 3.3\times 10^{-24} \left[\frac{E_{\text{H}}}{kT} \right]^{3/2} \times F_2(s) e^{-E_s/kT}/q_w \ , \tag{1}$$

where the rate coefficient for the satellite line $q(s)$ is given in terms of the parameter $F_2(s)$ which is determined by the autoionization and radiative decay rates for the dielectronic level s, i.e.,

$$F_2(s) = A_a(s) A_r(s) / [A_a(s) + A_r(s)] \ .$$

The q_w is the nonrelativistic, Maxwellian-averaged rate coefficient for the w line and $E_{\text{H}} = 13.6$ eV. Now, if we assume that a departure from the Maxwellian implies the excitation of the w line by relativistic electrons in the high-energy tail then, following Bartiromo *et al.*, one may define the fractional deviation from the Maxwellian as

$$\eta = \frac{q(w)}{q_{\text{rel}}(w)} \left[\frac{D_{\text{theor}}}{D_{\text{expt}}} - 1 \right] , \tag{2}$$

where $q_{\text{rel}}(w)$ is the relativistic excitation rate coefficient [Eq. (2) is a reformulation of the expression given by Bartiromo *et al.*].

As mentioned above, the assumption implicit in Eq. (2) is that the excitation of the w line depends only on the high-energy relativistic electrons. However, we adopt a somewhat different approach based on the concept of a bi-Maxwellian mentioned earlier. We write

$$T = aT_1 + (1-a)T_2 \ , \tag{3}$$

where a is the fraction of the electrons at the bulk temperature T_1 and $1-a$ is the fraction of nonthermal electrons, analogous to η in Eq. (2). The rate coefficient at T_2 is calculated by using the relativistic Coulomb-Bethe formula for the cross section given by Fano,

$$\sigma_w^{\text{rel}}(E) = \frac{8\pi a_0^2}{2E} \left[\frac{E_{\text{H}}^2}{E_w} \right] f_w \times \left\{ \ln \left[\left[\frac{\beta^2}{1-\beta^2} \right] (\bar{k}a_0)^2 \times \left[\frac{E_{\text{H}}}{E_w} \right]^2 \frac{2mc^2}{E_{\text{H}}} \right] - \beta^2 \right\} , \tag{4}$$

where f_w is the dipole oscillator strength, $\beta^2 = v^2/c^2$, and $\bar{k}$ is an averaged momentum transfer approximately $\approx Z/a_0$. For Ti XXI, we adopt the following values: $f_w = 0.7351$, $E_w = 4749.8$ eV, and $\bar{k} = 9.9/a_0$ to obtain

$$\sigma_w^{\text{rel}}(E,\text{eV}) = \frac{1.006\times 10^{-17}}{E} \times \left\{ \ln \left[60.38 \left[\frac{\beta^2}{1-\beta^2} \right] \right] - \beta^2 \right\} . \tag{5}$$

Finally, the relativistic excitation rate coefficient $\langle \sigma v \rangle_w$ at 10, 30, and 100 keV is calculated to be 6.16×10^{-12}, 6.78×10^{-12}, and 6.90×10^{-12} cm^3/s, respectively. As pointed out by Bartiromo *et al.* the energy variation in the relativistic rate coefficient is $\sim 10\%$. We therefore adopt a constant value of 6.5×10^{-12} cm^3/s for $T_2 > 10$ keV. We may now determine the quantity a in Eq. (3) from the expression

$$D_{\text{expt}} = \left[\frac{s}{w} \right]_{\text{expt}} = \frac{q(s)}{a q_w(T_1) + (1-a) q_{\text{w,rel}}(T_2)} \ . \tag{6}$$

Thus the observed ratio of the dielectronic to resonance line intensities yields the nonthermal fraction $1-a$. We label the method of Bartiromo *et al.* as (i) and ours as (ii).

In our observed spectra the satellite line j is quite accurately measured and we follow through the methods outlined above by studying the ratio j/w. In Table I the calculated values of the parameter η and $1-a$ are given as obtained from the two methods. The nonthermal content is related to the bulk temperature T_1 through the nonrelativistic, Maxwellian rate coefficient $q_w(T_1)$ that enters the calculation of $(j/w)_{\text{theor}}$. In using Eqs. (1) and (6), we have adopted the values $F_2(j)=3.53\times10^{14}$ from Ref. 25 and $E_j=3325.2$ eV. It is seen from Table I that our values for the non-Maxwellian component agree closely with those deduced by method (i) for the range of T_1 that we expect in the present plasmas. However, the fractional nonthermal component is quite considerable and much greater than expected. As a comparison, Bartiromo *et al.* have found that for the lower-hybrid rf pulse heating used in the Frascati tokamak the nonthermal component was less than 5%, while the Alcator C measurement[26] was $\sim0.1\%$ at high densities ($\bar{n}\sim0.7\times10^{20}$ m^{-3}). In the ECH case, fractions as high as 20—30% may be present.

In the analysis presented in this section we have considered it unnecessary to include the contribution from $n\geq3$ satellites to the resonance line for the following reasons. At the temperatures under investigation the $n=3$ satellites appear to be well separated from the main w line profile [the small, distinct hump to the right of the w line in Fig. 1(a)]. Regarding the $n>3$ satellites, while it is true that at low temperatures ($T_e<1$ keV) a significant fraction of the apparent resonance line intensity may come from these satellite lines, it is shown by Bitter *et al.*[27] that as the electron temperature increases their relative contribution decreases (about 10—15% at 1.4 keV for Fe XXV). In the present case the predominant excitation of the w line is caused by the very high-energy electrons produced during ECH [hence the good agreement between methods (i) and (ii)], and therefore the higher n satellites are expected to make a negligible contribution to its intensity (or at least within the uncertainties inherent in the theoretical techniques employed and the atomic data).

B. Bulk plasmas effects and input ECH power

The fact that the diagnostics based on the observed x-ray spectra appear to indicate a large non-Maxwellian component in ECH plasmas requires further consideration with a view toward obtaining at least an approximate, but independent, check. Elementary plasma kinetic theory yields the expression relating the input ECH power P into a plasma volume V, to the nonthermal high-energy electron density N_2, by the expression

$$\frac{dP}{dV}=\left[\frac{dT}{dt}\right]\frac{3}{2}N_2\ , \tag{7}$$

where

$$\frac{dT}{dt}=\frac{T_2-T_1}{t_{\text{eq}}}\simeq\nu_{\text{eq}}T_2\quad(T_2\gg T_1)\ , \tag{8}$$

where t_{eq} is the equilibration time[28] between the two electron distributions at T_1 and T_2, and the frequency ν_{eq} is its reciprocal. For $T_1\sim1$ keV and $T_2\sim10$ keV, we obtain $\nu_{\text{eq}}\simeq1.1\times10^3$ s^{-1} [Ref. 28, Eq. (5.30)]. The power $P_{\text{ECH}}=1$ MW$=10^{13}$ erg/s and the volume $V=2\pi(5\times10\times143)$ cm^3 (the last figure is the major radius of Doublet III). T_2 is a variable but if we restrict its range of values to 10—50 keV then we obtain $N_2\simeq(1.0-8.0)\times10^{12}$ cm^{-3}. Thus compared to the bulk electron density $N_e=N_1=(2-3)\times10^{13}$ cm^{-3}, the fraction N_2/N_1 is approximately in the range 0.03—0.40. Although these arguments are rather crude, it does appear that given the high input ECH power and its highly localized nature, the sharp deviations from a Maxwellian distribution indicated by the spectral diagnostics are quite possible.

Another approach to the determination of the suprathermal content based on plasma kinetic theory may be estimated as follows: The ratio η of superthermal electron density to the bulk Maxwellian electron density is approximately[29] $\eta\sim\nu_{\text{rf}}/\nu_c$, where ν_{rf} is the effective rf heating rate and ν_c is the electron-ion collision rate. Explicitly

$$\nu_{\text{rf}}=\frac{e^2E_-^2}{2^{3/2}m\Omega_0\epsilon T}\ , \tag{9}$$

and

$$\nu_c\equiv\tfrac{1}{2}\nu_{ei}Z_{\text{eff}}\left[\frac{m}{2T}\right]^{3/2}\ ,$$

here E_- is the magnitude of the right-hand-polarized rf electric field (corresponding to the extraordinary wave or x mode), Ω_0 is the rf frequency, ϵ is the ratio of the tokamak minor radius $a/2$ to major radius R, T is the

TABLE I. Fraction of suprathermal electrons. Note: the relativistic rate coefficient $q_{w_{\text{rel}}}(T_2)$ for Ti XXI is $\approx6.5\times10^{-12}$ cm^3 s^{-1} ($T_2>10$ keV).

T_1 (keV)	$q_w(T_1)$ (cm^3 s^{-1})	$(j/w)_{\text{expt}}$	$(j/w)_{\text{theor}}$	Method (i) η	Method (ii) $(1-a)$
0.8	3.16×10^{-14}	0.30	1.28	0.016	0.016
1.0	9.76×10^{-14}	0.20	0.68	0.036	0.037
1.2	2.01×10^{-13}	0.10	0.44	0.105	0.108
2.0	9.06×10^{-13}	0.05	0.14	0.250	0.290
3.0	1.90×10^{-12}	0.03	0.062	0.310	0.440

bulk electron temperature, $\nu_{ei}=4\pi n_0 e^4 \ln\Lambda/m^2$, and Z_{eff} is the effective ionic charge. The relation between the input ECH power P_{ECH} and the right-hand-polarized electric field E_- is given by $P_{\text{ECH}}=ACE_-^2/8\pi(k_\perp\rho_e)^2$ with A the effective heating area, $k_\perp$ the wave vector perpendicular to the magnetic field, and ρ_e the electron gyroradius (typically $k_\perp\rho_e\sim 0.1$). Finally, e, m, Λ, n_0, and c have the usual meanings.

For Doublet III, the parameters are $a=40$ cm, $R=143$ cm, $Z_{\text{eff}}\sim 2$, $\Omega_0=2\pi\times 60$ GHz, and $A\sim 2\pi(10\times 143)$ cm^2. The parameter η can be expressed as

$$\eta=0.47\frac{\sqrt{T}P_{\text{ECH}}}{n_0} \tag{10}$$

with T, P, and n_0 in units of 1 keV, 1 MW, and 10^{13} cm^{-3}, respectively. A plot of the calculated nonthermal fraction [Eq. (2)] as a function of the above scaling [Eq. (10)] is shown in Fig. 4. The parameters T, n_0, and P_{ECH} have been measured for each discharge. The points around 0.05 and above 0.4 on the x axis are the high ($n_0>1\times 10^{14}$ cm^{-3}) and low [$n\sim(2-3)\times 10^{13}$ cm^{-3}] density discharges, respectively. Between 0.1 and 0.2 the densities are about $(5-6)\times 10^{13}$ cm^{-3} and the nonthermal fraction variability is due mainly to the electron temperature, with the general rule that the higher electron temperatures correspond to larger η. The solid line is the scaling given by Eq. (10).

C. The principal lines of the He-like spectra

The intensities of the spectral lines, x, y, z, and w, relative to one another, are also an important source of high-temperature plasma diagnostics. For example, the line ratio G is sensitive to the temperature and, more strongly, to the ionization state of the plasma.[30] It is shown in earlier studies that this ratio is in the range 0.7–1.0 for the He-like ions in ionization equilibrium at temperatures close to the temperature of maximum abundance. For plasmas under dominant recombination conditions (cooling or colder parts of the plasma) the G values are considerably higher than 1.0. This is due to the fact that the recombination-cascade mechanism (see Ref. 30 for a detailed model) populates the $2\,^3S_1$ level preferentially and results in a large gain in the intensity of the z line.[20] On the other hand, we expect that a dominant nonequilibrium ionization state, e.g., rapidly heated or shocked plasma, would yield $G<0.7$. However, there is a lower bound on the G value given by the rates for electron impact excitation (EIE) of the levels $2\,^3S_1$, $2\,^3P_{0,1,2}$, and $2\,^1P_1$, i.e., $G_{\text{EIE}}<G$ where

$$G_{\text{EIE}}=\frac{q(2\,^3S_1)+q(2\,^3P_{0,1,2})}{q(2\,^1P_1)}\ ; \tag{11}$$

here the q are the rate coefficients for EIE from the ground state $1\,^1S_0$. Note that there are no recombination terms in Eq. (11); however, there may be a significant contribution to the G_{EIE} due to inner-shell ionization of the Li-like ionization stage resulting in the additional population of the $2\,^3S_1$ state, i.e., $1s^2(^1S)+e\rightarrow 1s2s(2\,^3S_1)+2e$. The Li-like stage burns up rather rapidly in a hot plasma but its presence should manifest itself in the enhanced intensity of the dielectronic satellite line q: $1s^2 2s\,^2S_{1/2}\leftarrow 1s2p2s\,^2P^\circ_{3/2}$ (which is subject mainly to the inner-shell excitation process) and, of course, in the enhancement of the line z.

In Fig. 3(a) we show the line ratio G as it varies during the ECH discharge. The observed range of values is 0.4–0.7 which indicates nonequilibrium ionization (recombination-cascade contributions to the $2\,^3S$ level are suppressed). We calculate the lower limit G_{EIE} given by Eq. (11) (from the rate coefficients tabulated in Ref. 31) to be $\simeq 0.4$. No values of this line ratio are observed to be significantly lower than G_{EIE}; indicating that no other processes, such as electron impact ionization out of the metastable level $2\,^3S_1$, are important. Also, this verifies the establishment of a theoretical lower bound on the ratio G, a fact that should prove useful in the analysis of the He-like spectra from other plasma sources.

The relative intensities of the lines x,y,z show quite anomalous behavior compared to the spectra in ionization equilibrium. Specifically, the ratio $R=z(x+y)$ is up to an order of magnitude lower than the equilibrium case [Fig. 3(b)]. R values as low as 0.1 are observed immediately at the onset of ECH, although the subsequent mean values are higher. This implies that relative to the enhanced w line (due to the high-energy electrons), the z line has diminished far more than the $x+y$ lines. This is apparent from the ECH spectrum in Fig. 1(a) which shows a very weak z line compared to equilibrium spectra. In equilibrium, such as usually achieved during Ohmic heating, the intensity of the z line for Ti XXI is approximately equal to the combined $x+y$ line intensities. The observations could have been explained readily had the electron density in the plasma been $\sim 10^{15}$ cm^{-3}, i.e., more than an order of magnitude higher than determined

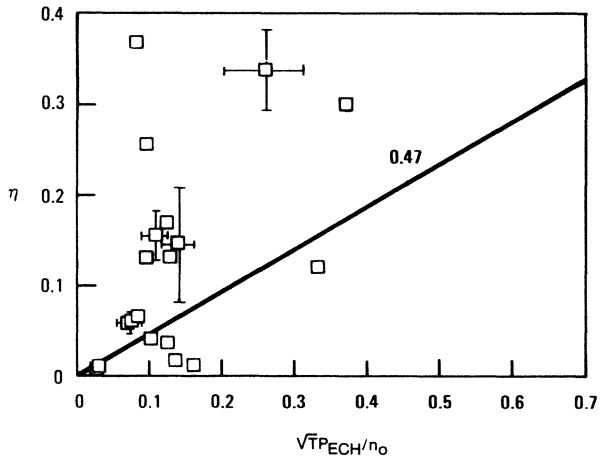

FIG. 4. The nonthermal fraction η as a function of the scaling $\sqrt{T}P_{\text{ECH}}/n_0$. The points between $0.1\le\sqrt{T}P_{\text{ECH}}/n_0\le 0.2$ have central densities $\sim(5-6)\times 10^{13}$/cm^3, however the higher electron temperature in general corresponds to larger η. Discharge-to-discharge variability is clearly evident. The straight line is given by Eq. (10). Nominal error bars for the data in each representation group are as shown.

by the laser interferometer and Thomson scattering techniques used to monitor the plasma during discharges. The $2\,^3S_1$ state can be collisionally coupled to the $2\,^3P_{1,2}$ states when the total excitation rate $q(2\,^3S_1 \rightarrow 2\,^3P_{1,2})$ is comparable to the radiative decay rate $A(2\,^3S_1 \rightarrow 1\,^1S_0)$, which is equal to 3.5×10^7 s^{-1}. We have calculated the relativistic rate coefficient for electron impact excitation of $2\,^3S_1$ level to the $2\,^3P_J$ levels using Eq. (4) and we find that at 30 keV these are the $q(2\,^3S_1 \rightarrow 2\,^3P_0) = 4.60\times10^{-11}$, $q(2\,^3S_1 \rightarrow 2\,^3P_1) = 1.30\times10^{-10}$, and $q(2\,^3S_1 \rightarrow 2\,^3P_2) = 2.19\times10^{-10}$ cm^3 s^{-1}, respectively (these rate coefficients are nearly twice the nonrelativistic values). In addition, the proton impact excitation rate from the $2\,^3S_1$ to $2\,^3P_J$ levels is approximately 10^{-9} cm^3 s^{-1}. It is therefore clear from these calculations that the total $2\,^3S_1 \rightarrow 2\,^3P_J$ excitation rate, at densities of $(2-3)\times10^{13}$ cm^{-3} (as measured for the present ECH plasmas), does not exceed 10^5 s^{-1}, about 2 orders of magnitude below $A(2\,^3S_1 \rightarrow 1\,^1S_0)$. At present there does not appear to be an explanation for the anomalously low z line intensity relative to $x+y$ (vignetting of the z line is not likely in the experimental setup), except perhaps the possibility that high densities might be present in the x-ray-emitting regions (other diagnostic apparatus measure only the averaged electron density and would not perhaps reveal information on such regions). Another possible reason may be the presence of another ionic impurity during ECH that might be opaque at the wavelength of the z line. We have not found any such impurity ions that might conceivably lead to this accidental, and highly selective, phenomenon.

ACKNOWLEDGMENTS

A.K.P. would like to thank Dr. F. Perkins and P.L. would like to thank Dr. J. Y. Hsu and Dr. K. Matsuda for discussions. This work was supported in part by the Department of Energy Office of Fusion Energy Grant No. EA-77-A-01-6010 (A.K.P.), and in part by National Aeronautics and Space Administration Grant No. NAGW-766 (Y.X.) and Department of Energy Contracts No. DE-AC03-84ER51044 and No. DE-FG02-84ER53189 (P.L. and A.J.L.).

[1]S. M. Wolfe, D. R. Cohn R. J. Temkin, and K. Kreischer, Nucl. Fusion **19**, 389 (1979).

[2]P. Prater *et al.*, GA Technologies Report No. GA-A17810, 1985 (unpublished).

[3]D. Farina, M. Lontano, and R. Pozzoli, in Proceedings of EC-4 Fourth International Workshop on Electron Cyclotron Emission and Electron Cyclotron Resonance Heating, Rome, 1984, (unpublished).

[4]D. A. Boyd, in Proceedings of EC-4 Fourth International Workshop on Electron Cyclotron Emission and Electron Cyclotron Resonance Heating, Rome, 1984 (unpublished).

[5]H. Hsuan *et al.*, Princeton Plasma Physics Laboratory Report No. PPPL-2114, 1984 (unpublished).

[6]See, for example, P. F. Winkler *et al.*, Astrophys. J. **246**, L27 (1981); C. Jordan and N. J. Veck, Sol. Phys. **78**, 125 (1982).

[7]M. Bitter *et al.*, Phys. Rev. A **29**, 661 (1984).

[8]M. L. Apicella, R. Bartiromo, F. Bombarda, and R. Giannella, Phys. Lett. **98A**, 174 (1983).

[9]J. E. Rice *et al.*, Phys. Rev. Lett. **56**, 50 (1986).

[10]E. V. Aglitskii *et al.*, Kvant. Elektron. (Moscow) **1**, 908 (1974) [Sov. J. Quantum Electron. **4**, 500 (1974)].

[11]R. Mewe and J. Schrijver, Astron. Astrophys. **65**, 115 (1978); **87**, 261 (1980).

[12]V. A. Bryzgunov, S. Yu. Luk'yanov, M. T. Pakhomov, A. M. Potapov, and S. A. Chuvatin, Zh. Eksp. Teor. Fiz. **82**, 1904 (1982) [Sov. Phys.—JETP **55**, 1095 (1982)].

[13]A. J. Lieber, S. S. Wojtowicz, and K. H. Burrell, Nucl. Instrum. Methods A **235**, 565 (1985).

[14]P. Lee, A. J. Lieber, and S. S. Wojtowicz, Phys. Rev. A **31**, 3996 (1985).

[15]K. Matsuda (private communication).

[16]K. Mutsuda, GA Technologies Report No. GA-A17689, 1985 (unpublished).

[17]A. M. Gabriel and C. Jordan, Mon. Not. R. Astron. Soc. **145**, 241 (1969).

[18]M. Bitter, K. W. Hill, N. R. Sauthoff, P. C. Efthimion, E. Meservey, W. Roney, S. Von Goeler, R. Horton, M. Goldman, and W. Stodiek, Phys. Rev. Lett. **43**, 129 (1979).

[19]E. Källne, J. Källne, and A. K. Pradhan, Phys. Rev. A **28**, 467 (1983).

[20]E. Källne, J. Källne, A. Dalgarno, E. S. Marmar, J. E. Rice, and A. K. Pradhan, Phys. Rev. Lett. **52**, 2245 (1984).

[21]D. L. McKenzie, R. M. Broussard, F. B. Landecker, H. R. Rugge, R. M. Young, G. A. Doschek, and U. Feldman, Astrophys. J. Lett. **238**, L43 (1980).

[22]A. H. Gabriel and K. Phillips, Mon. Not. R. Astron. Soc. **189**, 319 (1979).

[23]R. Bartiromo, F. Bombarda, and R. Giannella, Phys. Rev. A **32**, 531 (1985).

[24]M. Inokuti, Rev. Mod. Phys. **43**, 297 (1971).

[25]F. Bely-Dubau, P. Faucher, L. Steenman-Clark, M. Bitter, S. Von Goeler, K. W. Hill, C. Camhy-Val, and J. Dubau, Phys. Rev. A **26**, 3459 (1982).

[26]K. Kato and I. H. Hutchinson, Phys. Rev. Lett. **56**, 340 (1986).

[27]M. Bitter, K. W. Hill, M. Zarnstorff, S. Von Goeler, R. Hulse, L. C. Johnson, N. R. Sauthoff, S. Sesnic, K. M. Young, M. Tavernier, F. Bely-Dubau, P. Fancher, M. Cornille, and J. Dubau, Phys. Rev. A **32**, 3011 (1985).

[28]L. Spitzer, *Physics of Fully Ionized Gases*, 2nd ed. (Wiley-Interscience, New York, 1967).

[29]J. Y. Hsu *et al.*, Phys. Rev. Lett. **53**, 564 (1984).

[30]A. K. Pradhan, Astrophys. J. **288**, 824 (1985).

[31]A. K. Pradhan, Astrophys. J. Suppl. Ser. **59**, 183 (1985).